energies

MDPI

*Article*

# Intelligent Control of the Energy Storage System for Reliable Operation of Gas-Fired Reciprocating Engine Plants in Systems of Power Supply to Industrial Facilities

**Pavel Ilyushin [1,*], Sergey Filippov [1], Aleksandr Kulikov [2], Konstantin Suslov [3,4] and Dmitriy Karamov [1]**

[1] Department of Research on the Relationship between Energy and the Economy, Energy Research Institute of the Russian Academy of Sciences, 117186 Moscow, Russia
[2] Department of Electroenergetics, Power Supply and Power Electronics, Nizhny Novgorod State Technical University n.a. R.E. Alekseev, 603950 Nizhny Novgorod, Russia
[3] Department of Power Supply and Electrical Engineering, Irkutsk National Research Technical University, 664074 Irkutsk, Russia
[4] Department of Hydropower and Renewable Energy, National Research University "Moscow Power Engineering Institute", 111250 Moscow, Russia
* Correspondence: ilyushin.pv@mail.ru

**Abstract:** Gas-fired reciprocating engine plants (GREPs) are widely used in power supply systems of industrial facilities, which allows for ensuring the operation of electrical loads in case of accidents in the power system. Operating experience attests to the fact that during islanded operations, GREPs are shut down by process protections or protective relays in the event of severe disturbances. This leads to complete load shedding, which is accompanied by losses and damage to industrial facilities. Severe disturbances include the following ones: large load surges on GREPs due to one of them being switched off, the group starting of electric motors, and load shedding (more than 50%) during short circuits or disconnection of process lines. Energy storage systems (ESS) have the ability to compensate for instantaneous power imbalances to prevent GREPs from switching off. The authors of this study have developed methods for intelligent control of the ESS that allow one to solve two problems: prevention of GREPs shutdowns under short-term frequency and voltage deviations as well as preservation of the calendar and cycling lifetime of battery storage (BS) of the GREP. The first method does not require performing the calculation of adjustments of control actions for active and reactive power on the ESS online but rather determines them by the value of frequency deviations and the voltage sag configuration, which greatly simplifies the system of automatic control of the ESS. The second method, which consists in dividing the steady-state power/frequency characteristic into sections with different droops that are chosen depending on the current load of the ESS and the battery state of charge, and offsetting it according to a specified pattern, allows for preventing the premature loss of power capacity of the ESS BS.

**Keywords:** gas-fired reciprocating engine plant; industrial facility; off-grid energy areas; islanded operation; protective relay; electric motor; energy storage system; state of charge

**Citation:** Ilyushin, P.; Filippov, S.; Kulikov, A.; Suslov, K.; Karamov, D. Intelligent Control of the Energy Storage System for Reliable Operation of Gas-Fired Reciprocating Engine Plants in Systems of Power Supply to Industrial Facilities. *Energies* **2022**, *15*, 6333. https://doi.org/10.3390/en15176333

Academic Editor: Alan Brent

Received: 15 June 2022
Accepted: 28 August 2022
Published: 30 August 2022



## 1. Introduction

Many countries are phasing in long-term action plans to achieve carbon neutrality by 2050. This is possible either by reducing carbon dioxide emissions to zero or by maintaining a balance between emissions and removals, including through offsetting [1].

Therefore, in the electricity sector, the use of non-renewable energy sources is decreasing, and the construction of generating facilities based on renewable energy sources (RES) is increasing [2,3]. The great bulk of new generation capacity additions come from wind and solar energy, which in recent years have exceeded the volume of

capacity additions from conventional thermal, nuclear, and hydropower plants worldwide [4].

A distributed, low-carbon energy infrastructure, equipped with digital devices and systems, allows the most efficient use of all available types of primary energy resources [5,6]. An important precondition is to meet the needs of society for electricity, heating, and cooling in the necessary amounts and at affordable prices, as well as to ensure the reliability, availability, and safety of energy supply.

According to estimates by the International Energy Agency, decentralized energy can provide up to 75% of new consumer connections, as well as cover all of the needs to increase the capacity of electricity consumption by existing consumers in the future until 2030.

In order to minimize the negative impact on the environment and reduce greenhouse gas emissions, industrial facilities implement measures to utilize secondary energy resources [7]. Secondary energy resources include blast furnace gas, converter gas, mine gas, biogas from wastewater treatment plants, etc. Gas-fired reciprocating engine plants (GREP) of various manufacturers of a wide range of capacities have become widely used in this sector of the electric power industry [8,9].

Another factor encouraging industrial facilities to commission GREPs is the need to ensure reliable power supply and power quality at the buses of critical electrical loads involved in the continuous technological process [10,11].

Industrial facilities are usually powered by distribution grids, but it is possible for them to operate in an isolated state [12,13]. Additionally, the power supply system of an industrial facility may, for various reasons, be designed for islanded operation, with the load supplied by one or more GREPs. In these cases, the maintenance of active and reactive power balances must be provided entirely by GREPs [14].

Operating experience shows that under isolated or islanded operation, GREPs are shut down by protective relays (PR) during sudden load surges/dumps, which are caused either by technological process features or emergency disturbances. GREP shutdowns are related to their design features, the algorithms of automatic control systems (ACS) set, and the parameters of PR settings [15,16].

GREP shutdowns in most cases lead to disconnections of all electrical loads with the corresponding damage from emergency shutdowns and losses from lower manufacturing output by industrial facilities [17].

To solve a wide range of problems in the electric power industry, energy storage systems (ESS) have been widely used in recent years [18–20]. Given the high speed of the inverters, ESSs can effectively compensate for instantaneous imbalances of active and reactive power when they occur, preventing GREPs from shutting down.

An important issue in ensuring the reliable operation of the ESS together with the GREP is to maintain its state of charge (SoC) at an optimal level. Without an appropriate control algorithm, the ESS cannot perform this function to ensure the regulation of parameters of operating conditions within a given range, because the energy capacity of the battery storage (BS) of the ESS is chosen relatively small to minimize its cost [21,22].

The purpose of this article is to present the method developed by the authors for independent control of the active and reactive power of the ESS to prevent shutdowns of GREPs during short-term frequency and voltage deviations in isolated or islanded operation of the power supply system of an industrial facility. Furthermore, we present the method developed by us for maintaining the SoC of the ESS, which consists in segmenting the steady-state power frequency characteristic into individual sections with different droops and then offsetting it according to a specified pattern. This is necessary to prevent GREP shutdowns and ensure reliable power supply to critical electrical loads involved in the continuous technological process.

## 2. Overview of Causes of GREP Shutdowns and Ways to Prevent Them

As a rule, the maximum permissible short-circuit (SC) clearing time in power supply systems should not exceed 0.15 s. In the technical documentation that is shipped with GREPs, one of the manufacturers specified the following parameters for settings of protective relays whose action shuts down GREPs: voltage deviations in three phases above 110% or below 90% of $U_{nom}$ with a time delay of 0.2 s. Other manufacturers have the time delays of protective relays at a voltage drop ranging from 0.5 to 5 s, however, at the operation of backup protections, it is impossible to prevent shutdowns of GREPs [9].

In short-circuit/automatic reclosing (AR) cycles as well as when the automatic transfer switches (ATS) are triggered, which are accompanied by the self-starting of electric motors, short-term voltage drops are observed [23]. In the event of the above voltage dips and interruptions, GREPs are normally shut down by PRs.

As per the technical documentation supplied with GREPs by one manufacturer, parameters of adjustment of the GREP PR by frequency such that they lead to GREP shutdowns are as follows: frequency deviations above 51.5 Hz or below 49 Hz with a time delay of 0.2 s. Other manufacturers have GREPs shut down when the frequency rises above 55 Hz with a time delay of 4 s or when it falls below 47.5 Hz with a time delay of 2 s.

Short-term frequency and/or voltage deviations in the isolated or island operation of the power supply system are observed quite often. They can occur as a result of short circuits. Additionally, they can occur in certain circuit diagram configurations and operating conditions. For example, during the direct start of large electric motors or groups of electric motors of a single process line, as well as during disconnection of large electrical loads or their groups [24].

A design feature of the GREP is that it requires a greater air supply for normal operation: the more power it builds up the greater the air supply is required. When the shaft speed is reduced below the minimum allowable value the cylinders fail to provide the pressure necessary to ignite the air-and-fuel mixture in the compression phase.

Air is supplied to the GREP through a compressor, which is rotated by a compressor turbine, and its working medium is the exhaust gases from the GREP. At the load surge, the GREP ACS, due to a decrease in the shaft speed, increases the fuel supply, the GREP power goes up, and the amount of exhaust gases increases. In addition, the compressor and compressor turbine speed increases smoothly, ensuring the supply of larger amounts of air to the GREP [25].

The high moment of inertia of the compressor turbine/compressor system prevents rapid changes in the amount of supplied air, so the transition of the GREP to a higher power output state is delayed (about 1 s) relative to the electrical load surge. Delayed air supply during load surges leads to overheating of the GREP, so to prevent damage to the GREP, they are shut down by PRs [26].

It is important to note that the setpoints of GREP PRs set by their manufacturers are not subject to change without approval during the entire warranty period. If the owner of the GREP unilaterally changes the setpoints, the warranty obligations will be unilaterally canceled by the manufacturer.

The above approaches of GREP manufacturers to the choice of operation parameters of PRs lead to a narrowing down of the range of permissible operating conditions and GREP shutdowns, given the correct actions of PRs in the power supply system of an industrial facility. This creates emergency conditions for continuous technological processes.

Therefore, it is necessary to find such engineering solutions, the implementation of which would allow one to significantly reduce the number of GREP shutdowns under disturbances with short-term frequency and/or voltage deviations.

Let us list some examples of auxiliary engineering measures that should be implemented in the power supply system of an industrial facility:

- Maintaining the good working condition of electrical equipment to minimize the number of short circuits;
- Changing the network topology opening of sectional and bus coupling circuit breakers to minimize short circuit currents and the depth of voltage dips during short circuits [27,28];
- Bringing electrical equipment up to date: replacement of high-voltage circuit breakers with modern ones with a shorter intrinsic time of tripping in order to minimize the short-circuit clearance time, installation of current-limiting devices or isolation transformers to reduce the depth of voltage dips during short-circuits;
- Upgrading protective relays (use of fast-acting main and backup protections) and network automation (use of fast-acting ARs and ATSs);
- Using soft starters or variable frequency drives on large electric motors;
- Ensuring consecutive starts in groups of electric motors with voltage control on GREP buses or installing dynamic voltage compensators that provide reactive power injection to minimize the depth and duration of voltage dips.

However, the implementation of a large number of measures at an existing industrial facility can take quite a long time, and, moreover, will require significantly larger financial outlays.

The most effective solution, which can be implemented quickly, is the installation of an ESS. This will compensate for momentary imbalances of active and reactive power that cause short-term frequency/voltage fluctuations and prevent GREPs from shutting down.

## 3. Overview of Ways to Maintain the State of Charge of the ESS

The following operating conditions of the ESS are known, the choice of which is conditioned by the tasks to be solved: $U/f = const$, $PQ$-control, operation with steady-state power frequency, and/or power/voltage characteristic [29,30].

In the $U/f = const$ (voltage source) mode, the ESS maintains the frequency and voltage in the power supply system regardless of the current values of active and reactive power generation by GREPs, acting as the master inverter. The ESS ACS sets the amount of active and reactive power generation necessary to maintain the frequency and voltage within the specified setpoints, thus implementing overall primary regulation.

In the $PQ$-control mode (current source), active and reactive power generation by the ESS is kept constant if the frequency and voltage are within the range of permissible conditions. Consequently, the ESS is not involved in the overall primary regulation. $P$ and $Q$ setpoints are set either by the ESS ACS or by the power system ACS, which allows the ESS to participate in the secondary frequency and voltage regulation [31].

If the ESS operates with a steady-state power frequency and/or power/voltage characteristic, it facilitates frequency/voltage regulation conditions in the isolated or islanded operation of the power system for other GREPs by participating in secondary frequency/voltage regulation [32].

Regardless of the chosen operating conditions of the ESS, an important aspect of its operation is to keep the SoC at an optimal level. At the extreme values of the SoC (0% or 100%), there are no possibilities for the ESS to participate in regulating the parameters of operating conditions. The studies [33,34] consider various ways to maintain the SoC of the ESS.

The first group of them includes methods for ESSs that implement the function of the master inverter, in which the dedicated GREP for maintaining SoC receives information about the current value of SoC through the data link. This information is received by the ACS of the GREP, and the power of the GREP is set in proportion to the deviation of SoC from the specified value. This approach makes it possible to ensure high accuracy in maintaining the mean value of SoC, with the relative simplicity of implementing the algorithm in the ESS ACS.

The disadvantages of this method include the fact that the capacity of the ESS inverter must be designed for 100% of the load in the power supply system. In addition, it is necessary to create a data link from the ESS to GREP, and its damage leads to the SoC value exceeding the permissible range, as well as requires reconfiguration of the GREP ACS for interaction with the ESS.

The second group includes the methods that do not use the data link between the ESS ACS and the GREP ACS and are based on the application of the steady-state power frequency characteristic. In [35–37] it is proposed to change the slope of the steady-state power frequency characteristic of the ESS according to a specified pattern. In this case, in the discharge/charge processes, the ESS will produce/consume more or less active power [38–41]. This approach is effective for aligning SoCs that operate in parallel.

In [42–45] it is proposed to offset the steady-state power frequency characteristic of the ESS along the frequency axis, depending on the SoC, while the ESS discharge/charge processes will change the intensity of the response to frequency changes. This approach has high reliability in maintaining the specified SoC value, provides the possibility of parallel operation of several ESSs with the same SoC values, and does not require reconfiguration of the GREP ACS.

The disadvantages of this method include the fact that the ESS is not involved in the overall primary frequency regulation but only in the secondary frequency regulation. In this case, the SoC value is maintained within a permissible range rather than near the specified value. At the same time, the ESS ACS has a more complex structure and algorithms.

## 4. Key Defining Features of Circuit Diagram Configurations and Operating Conditions of GREP Operation and the Choice of ESS Parameters

Isolated or islanded operation of the power supply system of an industrial facility with GREPs under various circuit diagram configurations and operating conditions has markedly distinct features. All circuit diagram configurations and operating conditions can in principle be divided into two groups:

- At the beginning of the transient, the voltage is undervoltage due to a short circuit or connection of a group of motors with slips much larger than normal. Self-starting or group starting of electric motors in many cases require additional reactive power generation, which should be taken into account when choosing parameters for the ESS;
- At the beginning of the transient, the voltage is close to the nominal value, so there are no conditions for braking the motors. If a shortfall of active power occurs and it is necessary to increase the frequency to the nominal value while preventing the shutting down of the GREP PRs, then under-frequency load shedding (UFLS) devices should be used and, as a supplement, the ESS should be used.

The first group includes circuit diagram configurations and operating conditions arising in the case of triggering of ATS devices with a dead time of 2–3 seconds. Maintaining the reactive power balance by ESS is economically not feasible. It is necessary to apply control actions (CA) to load shedding (LS) and after normalization of operating parameters by the action of special automatics, which is to ensure successive starts of small groups of electric motors.

The second group includes circuit diagram configurations and operating conditions occurring when one or more of the GREPs that are switched on are suddenly switched off. If the total available capacity of the GREPs remaining in operation, taking into account their overload capacity, is insufficient to maintain the balance of active power, it is necessary to implement LS CAs:

- With the use of UFLS devices that have a frequency setpoint higher than $f_{min}$ of the GREP PRs. In this case, the LS value must not be less than the power of the largest of the GREPs switched on, if their powers are different. Experience attests to the fact

that implementing LS by the action of UFLS devices leads to the need to disconnect a larger amount of load, which proves critical for industrial facilities. This is due to the fact that UFLS devices have a time delay of 150–300 ms, and with a high rate of frequency reduction during islanded operation, their speed may not be enough;

- With the use of a special automatic load shedding system (SALSS), which acts when one or more GREPs are switched off and records the actual value of the disconnected generated active power using a device for monitoring prior operating conditions. The implementation of the LS CA should be carried out when a specified frequency set-point is reached.

Let us consider a simplified single-line diagram of the power supply system of an industrial facility with several GREPs as shown in Figure 1.

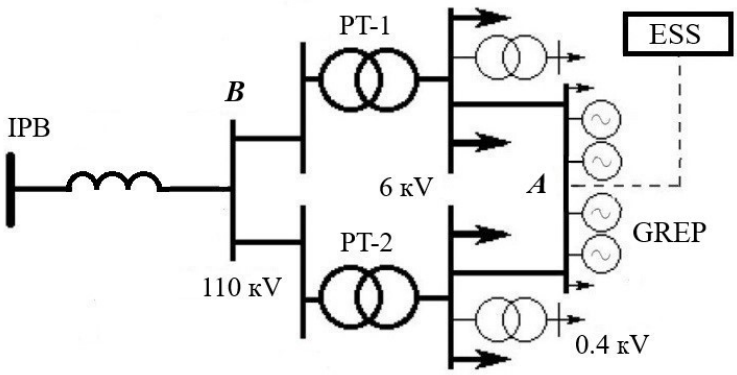


**Figure 1.** Simplified single-line diagram of the power supply system of an industrial facility with several GREPs.

In Figure 1, the infinite power bus (IPB) shows all external sources of equivalent unchanged electromotive force (EMF) behind a resistance corresponding to the short-circuit power. Electricity consumption in the power supply system of an industrial facility—20 MW, and the total capacity of the GREP—10 MW. Power consumed by electrical loads as percentages of the total value: synchronous motors—10%, asynchronous motors (AM)—62%, static load—28%. The parameters of the equivalent AMs differ: $M_{stat}/M_{nom}$ = 0.2 (for AMs accounting for 20% of their total consumption), 0.4 (70%), and 0.8 (10%), respectively. The total power of the operating GREPs in the transient calculations varied. The CA is applied to the ESS connected to the GREP buses at node ***A*** (Figure 1).

GREPs are equipped with standard synchronous generators. The difference lies in the use of a gas-fired reciprocating engine to drive the synchronous generator, which differs from the steam or gas turbine in several key ways. The difference is in the maneuvering characteristics of the GREP: the allowable load surge value and the time between successive load surges. Modern gas-fired reciprocating engines are equipped with a turbo-supercharging system, which provides the necessary amount of air into the combustion chambers when the load on the synchronous generator changes. Air is supplied to the gas-fired reciprocating engine through a compressor, which is rotated by a compressor turbine, and its working medium is the exhaust gases from the GREP. The high moment of inertia of the compressor turbine/compressor system prevents rapid changes in the amount of turbo-supercharging, so the transition of the GREP to a higher power output state occurs with a delay (at least 1–2 s) relative to the electrical load surge. If the load surge is greater than the allowable value (at an initial load of 60% it is no more than 10–15%) GREP will be switched off either by process protection or by synchronous generator frequency reduction protective relays. To prevent GREP from switching off during short-term frequency and voltage deviations in islanded operation of the power supply system, the ESS is used.

Figure 2 shows the results of calculations of transients when one of the four GREPs is switched off by the process protection (without short-circuit) $P_{GREP\ nom}$ = 2.5 MW. Additionally, the total load in the power supply system is $P_{load}$ = 9.2 MW in the islanded state, with losses factored in. Before the shutdown, this GREP was generating about 2.5 MW, while the other three GREPs were generating 2.24 MW each.

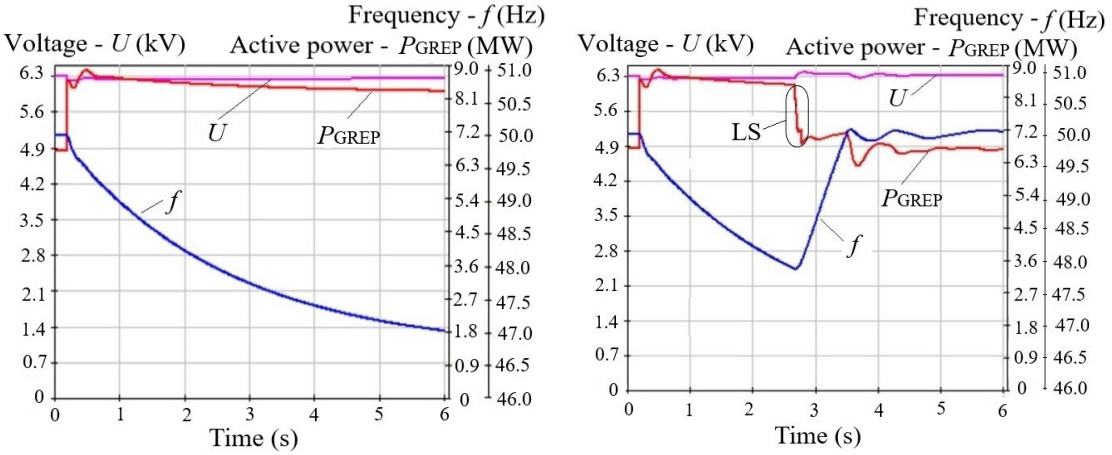


**Figure 2.** Transients in the event of shutting down one of the four GREPs: (**a**)—without applying the LS CA; (**b**)—with the action of SALSS ($P_{GREP}$—power of 3 operating GREPs).

If one chooses not to apply an LS CA, then the power supply system sets $f$ = 46.7 Hz (Figure 2a) with the frequency regulation droop close to zero (the available power of the switched-on GREPs is equal to 110%). If in the case of disconnection of one GREP and frequency decreases down to $f$ = 48 Hz by the action of the SALSS the CA is applied in the amount of 2.5 MW step-wise within 0.1 s, the frequency is restored up to $f$ = 50.0 Hz (Figure 2b). The action of the SALSS is a response to shutting down the GREP before the frequency reduction allows one to minimize the amount of LS, thus preserving the power supply to a greater number of electrical loads.

If the shutting down of a single GREP occurs as a result of a short-circuit, then during the transient process the remaining GREPs may be shut down by the action of the PRs because of a short-term voltage drop, if their setpoints are close to $U_{nom}$ and the time delay is less than the allowable short-circuit duration.

It is not economically feasible to apply CAs to the ESS to increase the voltage at the GREP buses until the short-circuit is cleared, because significant amounts of reactive power will be required. To reduce short-circuit clearing time it is necessary to reconstruct the protective relays, with the installation of high-speed protections, both in the distribution grid and in the power supply system of an industrial facility. It is often effective to install current-limiting devices to reduce the depth of voltage dips at the GREP buses during short circuits in the electrical distribution network.

Voltage control in power systems is realized by two methods:

- Regulation proportional to deviations of the current voltage value from the specified value (with possible use of signals, including those proportional to time derivatives of operating conditions parameters);
- Discrete boost, with two levels of reactive power output: normal and boosted.

The magnitude of the control error is much smaller. However, the connection to the ESS GREP buses with the ACS, in which the control algorithm is implemented, may require them to be reconfigured in a joint fashion. This is important to avoid oscillatory instability under different circuit diagram configurations and operating conditions, as well as to ensure good damping of oscillations in case of disturbances. High accuracy is

not required to solve the problem of voltage maintenance with the aid of ESS at GREP buses.

The reactive power control of the ESS as per the boosting principle is the simplest and most effective solution. In this case, the ESS does not output reactive power as normal but delivers the maximum amount of reactive power when the voltage drops below the specified setpoint. The boosting mode can be set at different voltage values by the value of reactive current $I_{CA}$ or reactive power $Q_{CA}$.

If the parameters of operating conditions during a transient are close to normal values, it is necessary to reduce the CA on the ESS with respect to $I_{CA}$. This is to be completed at the end of the self-start of electric motors due to a significant decrease in the value of the current consumed by them. Otherwise, a voltage increase above $U_{max}$ is possible, which will cause the GREP to shut down by the overvoltage protection. If, on the other hand, in the ESS ACS it is not $I_{CA}$ but $Q_{CA}$ that is set, then when the voltage rises, $I_{CA}$ will decrease without additional actions. In the calculations of the transients given in this article, this is the method adopted for applying CAs [46].

One should not withdraw the CA on the ESS as long as there is a possibility of repeated braking of the electric motors with a corresponding voltage drop. On the other hand, when most motors have reached normal speed, the excessive reactive power output causes the voltage to rise. Analysis of the results of transient calculations showed that the optimum voltage of the CA withdrawal is approximately equal to the nominal voltage of the network to which the GREPs are connected. In the calculations presented in the article, the bus voltage at which the CA acting on the ESS is withdrawn is 6 kV.

The specifications of the ESS should be chosen with the following in mind:

- ESS should contribute to the normalization of parameters of operating conditions after the elimination of an emergency disturbance to prevent GREP shutdowns, as well as to ensure the successful self-starting of electric motors in the power supply system of an industrial facility;
- Considering the effect of the ESS on the operating conditions of the entire power supply system, in order to minimize its power and energy intensity it is necessary to simultaneously implement additional engineering measures, a list of which is given above;
- A check of the possibility of disconnection of GREPs by PRs must be performed for all types of emergency disturbances, including remote ones (for example, non-synchronous AR on power supply lines; short circuits at the buses of adjacent substations; load surges/dumps in the power supply system, etc.), with a high probability, and not only for the most severe disturbance (nearby three-phase short circuit);
- A check of the possibility of disconnection of the GREP by PRs should be performed under asymmetric emergency disturbances as well as under post-emergency voltage asymmetry.

Requirements for the formation and application of CA to the ESS to prevent shutdowns of the GREP:

- It is necessary to introduce the CA quickly in a way appropriate to the circuit diagram configurations and operating conditions (implementation time not more than 30 ms) that indicate the occurrence of such operating conditions where it is possible for the GREP to be shut down by the PRs;
- CA introduction until the multiphase short-circuit is cleared is of no effect, especially for nearby short-circuits;
- Taking into account the nature and parameters of the transient, it may be necessary to reapply the CA to the ESS; in such case starting up is triggered by a deviation of the monitored parameter, for example, by a voltage drop;
- The output of active/reactive power of the ESS during the transient should be performed at the current frequency value (ESS frequency control is what is being controlled) to eliminate an increase in complexity of the ESS ACS [47].

Calculations of transients were performed with the aid of the MUSTANG-90 software package (Russia) for various circuit diagram configurations and operating conditions in the power supply system of an industrial facility with GREPs. The calculations attested to the efficacy of the methods developed by the authors.

## 5. Method for Independent Control of Active and Reactive Power of the ESS

Preventing the shutdowns of GREPs by PRs during short-term frequency deviations is especially relevant in isolated or islanded operations of the power supply system. This is due to the small values of the mechanical constant of inertia of the GREP, the lag of air supply to the GREP, as well as setpoints of protections with respect to $f_{min}$ and $f_{max}$, close to $f_{nom}$ = 50 Hz.

Let us list the features of the method developed by the authors for independent control of active and reactive power of the ESS, aimed at stabilizing the frequency in the power supply system of an industrial facility with GREPs:

1. When the balance of active power in the power supply system is disturbed and is accompanied by a frequency deviation from $f_{nom}$, CAs are applied to the ESS. CA adjustments are chosen so that the frequency does not go beyond a range narrower than the range of frequency values, as specified by the setpoints of GREP PRs.
2. The choice of CA adjustments applied to the ESS is specified differently for the initial stage of the transient (emergency disturbance) and for the intermediate points of the transient at unsteady parameters of operating conditions.
3. At the initial stage of the transient, when a rapid change in the GREP active power output ($\Delta P_{GREP}$) is observed, it is necessary to ensure with minimum delay the application of the CA to the ESS with respect to the active power ($CA_{ESS\text{-}P}$) in the amount of $\Delta P_{ESS} \approx \Delta P_{GREP}$. It is difficult to perform a direct measurement of $P_{GREP}$ in a transient because switching in the power supply system causes rapid changes in the subtransient and aperiodic components of currents as well as their harmonic components due to individual phase imbalance. Measuring the correct value of $P_{GREP}$ can lead to performance degradation in the event of applying $CA_{ESS\text{-}P}$.
4. The application of $CA_{ESS\text{-}P}$ at the initial stage of the transient in the amount of $\Delta P_{ESS} \approx \Delta P_{GREP}$ should be carried out in proportion to the frequency derivative given islanded operation of the power supply system:

$$\Delta P_{ESS} = -K_{df} \cdot (df/dt)_0, \quad (1)$$

where $K_{df}$ is the coefficient of proportionality. Calculation of $K_{df}$ is performed when loads of different magnitudes are connected to GREPs, recording the value of load increment on the GREP ($\Delta P_0$) and the frequency derivative $(df/dt)_0$ (Figure 3).

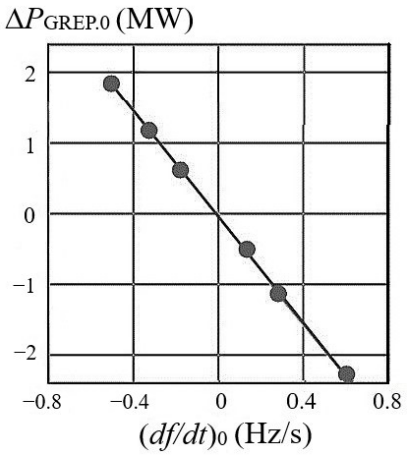


**Figure 3.** Graph of the relationship $\Delta P_{GREP.0} = \varphi(df/dt)$ in the power supply system with GREPs ($K_{df}$ ≈ −3.74 MW·s/Hz).

The graph of the relationship $\Delta P_{GREP.0} = \varphi(df/dt)$ in the power supply system with GREPs (Figure 3) is obtained for the considered power supply system of the industrial facility, the process flow diagram of which is shown in Figure 1. For some other power supply systems in islanded operation, such a graph will have to be obtained on a case-by-case basis, taking into account the GREP per-unit capacity based on contingency calculations of transients. Figure 3 corresponds to an emergency disturbance with the shutdown of a single GREP.

5. In the transient with load surge at GREPs, the unambiguous correspondence between $\Delta P_{GREP}$ and $df/dt$ is broken due to the influence of dynamic power components, so the $CA_{ESS\text{-}P}$ should be implemented differently. In addition, the boundary values of frequency $f_1$, $f_2$ are set to implement frequency control in the power supply system, in addition to $f_{min}$, $f_{max}$, which characterize the setpoints of the GREP PRs, as follows:

$$f_{min} < f_1 < f < f_2 < f_{max}. \quad (2)$$

6. In order to control the transient, the ESS ACS monitors the frequency in the power supply system at equal time intervals T. If $f < f_1$, it outputs a CA to increase $P_{ESS}$ so as to reduce the load at the GREP and increase the frequency. If $f > f_2$, it outputs a CA to reduce $P_{ESS}$. Optimal values of intervals $T$ and ESS power steps ($+\Delta P_{ESS}$, $-\Delta P_{ESS}$) are chosen based on the results of transient calculations.
7. It is possible to increase the efficiency of ESS control if the values of power steps ($+\Delta P_{ESS}$, $-\Delta P_{ESS}$) are changed in proportion to the current values of the frequency derivative in the power supply system $(df/dt)t$.
8. After completion of the controlled part of the transient, when there is no need to change $\Delta P_{ESS}$ within 6–10 s, i.e., $f_1 < f < f_2$, the ESS ACS smoothly (or in several steps) zeros out the value of $CA_{ESS\text{-}P}$. After that, the ESS SoC recovery algorithm is launched.
9. Since in isolated and islanded operation during surges of active load at the GREP, the frequency in the power supply system decreases for a short time, when choosing the $CA_{ESS\text{-}P}$ adjustment it is necessary to factor in the value of the power frequency characteristic to reduce the amount of active power imbalance.

Let us consider the results of calculations of transients in which the GREPs were not shut down by the PRs in the islanded operating state, due to the application of a CA to the ESS with respect to active and reactive power.

The following setpoints of the PRs with respect to the frequency of the GREP are set: $f_{min}$ = 47.5 Hz with a time delay of 2 s, $f_{max}$ = 55 Hz with a time delay of 4 s. To control the power of the ESS the boundaries of the range of permissible values are set as follows: $f_1$ = 49, $f_2$ = 51 Hz. It is taken into account that violation of the condition $f_1 < f < f_2$ is permissible for a time shorter than the time delay of the GREP PRs. $T$ = 300 ms was assumed in the calculations (changes in the range of 200–500 ms have no effect on the calculation results), and $\Delta P_{ESS}$ steps are +10% and −20% of the preceding value of active power.

In the calculations of transients, it was assumed that at the initial stage of the transient the control of the active power of the ESS is introduced with a delay of 60 ms (triggering of the starting element; calculation of $(df/dt)_0$ and $\Delta P_{ESS}$; taking over the CA by the ESS ACS), subsequent control with respect to frequency smaller than $f_1$ or larger than $f_2$ is performed with a delay of 30 ms.

Let us consider examples of $CA_{ESS\text{-}P,Q}$ application, where in fundamentally different transients with severe disturbances, the method developed by the authors for ESS control allows one to prevent GREPs shutdown while having the same CA adjustment. Consequently, an important advantage of this method is the possibility to determine the CA adjustment as applied to the ESS by the magnitude of frequency deviations, without the need for online calculations.

1. *Load surge at GREPs during group starting of electric motors.*

Figure 4 shows the calculation of the electromechanical transient during islanded operation of the power supply system operating under minimum load conditions Under

such conditions, a group of electric motors with a total capacity of 0.94 MW (37.5% of $P_{GREPnom}$) must be started from one running GREP. Taking into account the factory-set set-points of the GREP protective relay for frequency reduction, without employing the ESS, it is possible to successfully implement the direct starting of electric motors with total power not more than 0.25 MW (10% of $P_{GREPnom}$). Since the process flow of the industrial facility requires performing simultaneous direct starting of electric motors with a total capacity of 0.94 MW (there are no soft starters and variable frequency drive for electric motors), it can be implemented only through the use of the ESS. "Sawtooth" characteristics are due solely to the active power control algorithm of the ESS. Given the speed of the ESS inverter, which implements the CA in about 10 ms, the transient graph (one-second range) shows it as "sawtooth" characteristics.

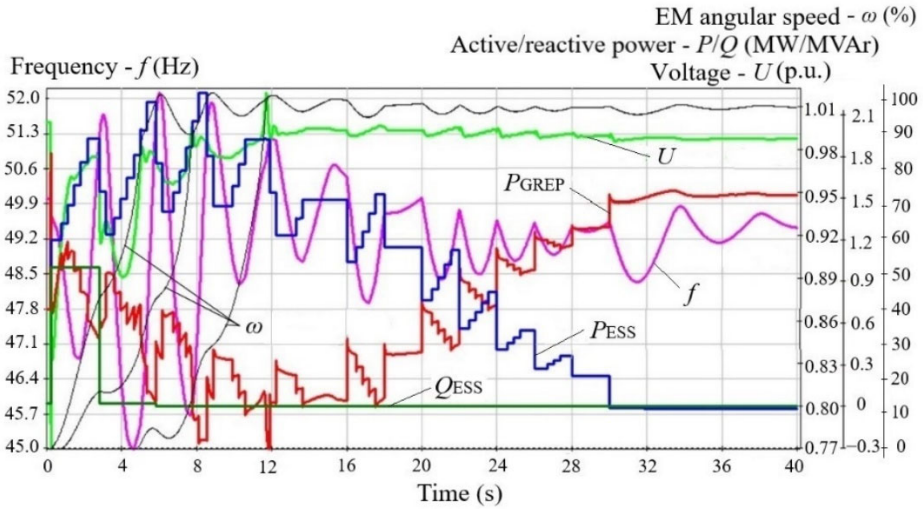


**Figure 4.** Transient in the case of a group starting of electric motors by a single GREP.

In the baseline mode, the load of the GREPs is 30% of $P_{GREPnom}$. The total nominal power of electric motors during group starting is 37.5% of $P_{GREPnom}$. The results of the calculation of the transient given a group start of electric motors by a single GREP, with the application of the CA to the ESS with respect to $P$ and $Q$ according to the method developed herein, are shown in Figure 4.

Analysis of Figure 4 shows that the application of the CA to the ESS with respect to $P$ and $Q$ makes it possible to provide successful group starting of electric motors of large total power in islanded operation without switching on additional GREPs. Such conditions can occur at minimum power consumption at an industrial facility when one of the four GREPs remains in operation.

2. *Shedding 95% of the load from the GREP at nominal initial load.*

Under the baseline conditions, the load of the GREP is 100% of $P_{GREPnom}$. The load shedding from the GREP is 95% of $P_{GREPnom}$. In this case, there is a transient process with a significant short-term increase in frequency, at the beginning of which the CA are applied to the ESS in the amount of active power consumption equal to the value of load shedding $\Delta P_{ESS} = -2.3$ MW (Figure 5).

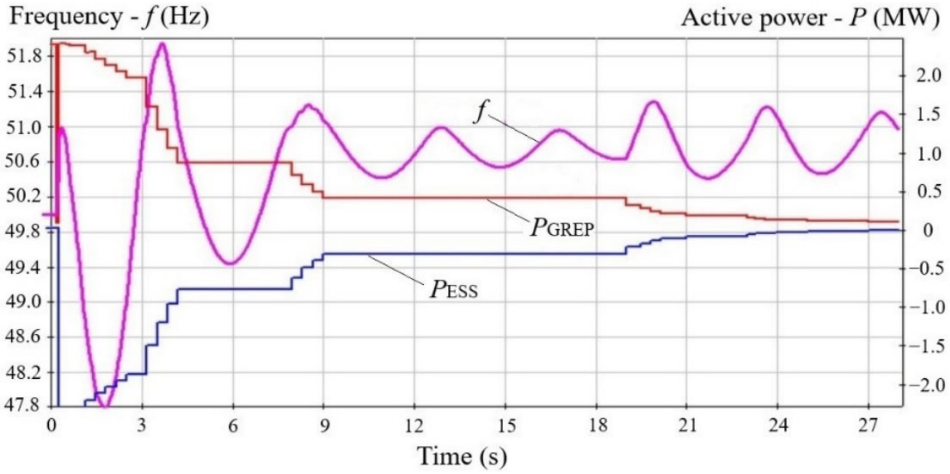


**Figure 5.** Transient in the case of shedding 95% of the initial GREP load.

If large power drops occur quite often at an industrial facility, then in the ACS of the ESS under normal operating conditions an algorithm must be implemented to maintain such a value of the ESS SoC that would allow operating with the power $+\Delta P_{GREPnom}$. Such operating conditions can occur, for example, when a large process line is shut down.

The analysis of Figure 5 shows that the application of the CA to the ESS with respect to *P*, in accordance with the method developed, makes it possible to prevent the GREP shutdown in the case of shedding 95% of $P_{GREPnom}$, accompanied by a short-term increase in frequency under islanded operating conditions. This makes it possible to provide a reliable power supply to the remaining electrical loads in operation [48,49].

3. *Three-phase short circuit in the power supply system with GREPs.*

In the baseline mode, the load of the GREP is 2.24 MW. As a result of a three-phase short circuit in the power supply system of an industrial facility, the power supply to electrical loads with a capacity of 27% of $P_{GREPnom}$ is disrupted. Next, in 0.38 s, the power supply to the disconnected electrical loads is restored by the action of the ATS device. The transient during this emergency disturbance is shown in Figure 6.

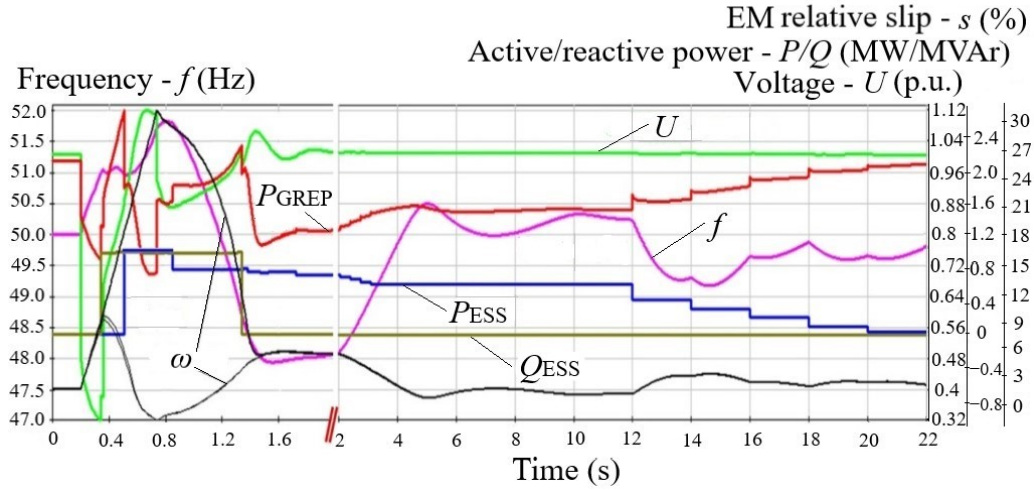


**Figure 6.** Transient at three-phase short-circuit in the power supply system with GREPs.

The analysis of Figure 6 shows that this transient differs from the other two (Figures 4 and 5) in that the use of a higher-power ESS increases the efficacy of control. There are no general patterns in this case, because at different depths of voltage dips, short-circuit duration, and different load parameters, the optimal adjustments of the CA applied to the ESS will be different. The choice of the adjustments of CAs applied to the ESS with respect

to $P$ and $Q$ should be made on the basis of the results of the analysis of short-circuit probabilities with the use of standard means of increasing the dynamic stability of the load.

Establishing technical specifications for the ESS should be based on the results of calculations of transients. The analysis of the transients shown in Figures 4–6 made it possible to establish the requirements for the ESS, which are shown in Table 1 ($p > 0$ when the ESS power is delivered).

**Table 1.** Specifications to be met by the ESS in the power supply system with GREPs.

| Figure | $U_{nom}$, кV | $I_{max}$, A | $P_{max}$, MW | Energy Intensity ESS, MW·s |
|---|---|---|---|---|
| Figure 4 | 6.3 | 220 | +2.1 | +25 |
| Figure 5 | 6.3 | 220 | –2.4 | –12 |
| Figure 6 | 6.3 | 130 | +1.0 | +10 |

The presented method allows one to minimize the requirements for power and energy intensity of the ESS BS, and hence the cost of the ESS. This was made possible by maximizing the use of the GREP overload capacity, since the implementation of the CA applied to the ESS is chosen so as to take into account the GREP protective relay setpoints with respect to frequency.

It is possible in principle to increase the voltage at the buses of GREPs to prevent them from shutting down by applying a CA to the ESS with respect to $Q$. However, as long as the multiphase short-circuit is not cleared, it is possible to increase the voltage only when having the power $Q_{CA}$ significantly higher than the power of the short-circuit. In addition, the output of a significant amount of reactive power from the ESS at the moment of a short circuit can significantly increase the value of the short-circuit current. This may be unacceptable due to the insufficient breaking capacity of high-voltage circuit breakers or will lead to shortening their electrical lifespan at an accelerated pace.

Consequently, the voltage control by applying CAs to the ESS with respect to $Q$ is effective when implemented immediately after clearing the short circuit. If the short-circuit durations are such that the GREP PR used to lower voltage can trip during the short circuit, then the reactive power output from the ESS is of no effect. Therefore, the reduction of the short-circuit clearing time by replacing the PRs and high-voltage circuit breakers is the only engineering solution. If the time delay of the protection by voltage drop at the GREP is 0.5–5 s, which is triggered in the process of self-starting electric motors in the load, then applying the CA to the ESS with respect to $Q$ is feasible.

Figure 7 shows the results of calculations of transients at a three-phase short-circuit at node ***B*** when four GREPs are in operation (Figure 1). For comparison, four calculations of transients are given: without applying the CA, as well as with applying the CA to the ESS with respect to $Q$ after clearing the short circuit. The value of $Q_{CA}$ = 10 MVar, and the duration of the CA varies. In Figure 7: $\Delta U$—increase in the voltage at GREP buses in case of applying the CA to the ESS; $\Delta t$—the time during which the voltage at GREP buses is below $U_{min}$ = 5.67 kV (90% of $U_{GREPnom}$ = 6.3 kV); blue arrows indicate the time during which the voltage is below $U_{min}$.

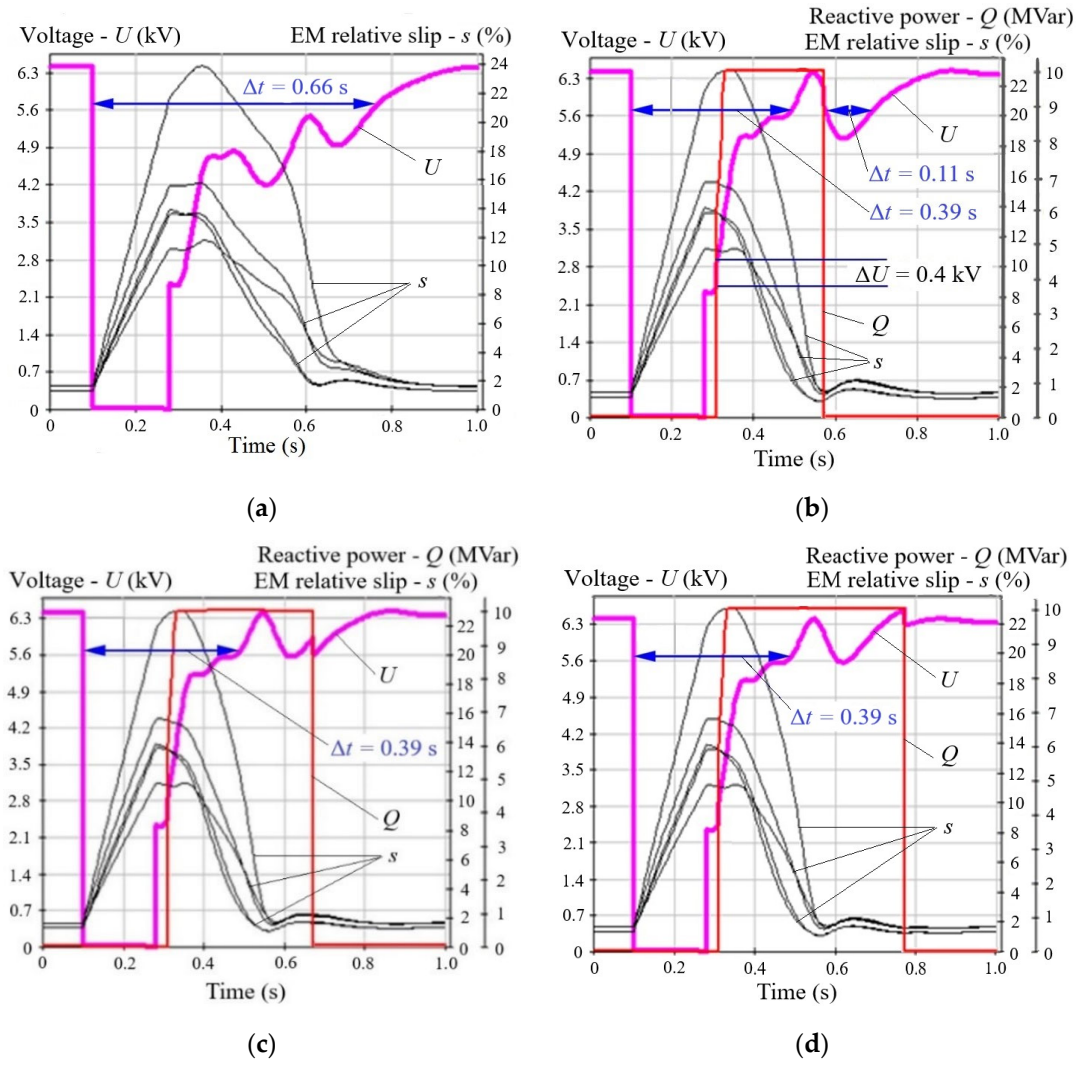


**Figure 7.** Transients during a three-phase short-circuit: (**a**)—without applying the CA to the ESS; (**b**)—withdrawal of the CA from the ESS when $U_{GREPnom}$ is reached; (**c**)—withdrawal of the CA from the ESS with a time delay of 0.1 s; (**d**)—withdrawal of the CA from the ESS with a time delay of 0.2 s.

In the method developed, the control of the ESS with respect to $Q$ is implemented as per the principle of boosting the excitation of generators: $\Delta Q_{ESS} > 0$ if $U < U_{min}$. The values of these parameters are chosen on the basis of preliminary results of transient calculations. In the transients shown in Figure 7, the CA applied to the ESS with respect to $Q$ was introduced in 30 ms after clearing the short circuit, and the response time of the ESS was assumed to be 5 ms.

The analysis of Figure 7 shows that the duration of the CA applied to the ESS has no significant effect on $\Delta t$ if it is not less than the duration of self-starting of the main electric motors in the power supply system. At the same time, the application of the CA to the ESS with respect to $Q$ allows one to prevent GREP shutdowns.

The magnitude of the instantaneous voltage rises at the moment of applying the CA to the ESS ($\Delta U$) depends on the extent of the CA ($Q_{CA}$) and is close to linear for different load compositions. The decrease in time $\Delta t$ is more noticeable, the greater the available power $Q_{CA}$, and the greatest effect is obtained when $Q_{CA}/P_{GREP} \approx 0.4$–$0.5$. Parameters that have a significant effect on the value of $\Delta t$ are the relative power $P_{GREP}/P_{load}$ and the short-circuit power at GREP buses.

The method developed by the authors for independent control of active and reactive power of the ESS differs from the known ones by the fact that it does not require performing calculations of CA adjustments applied to the ESS online. We propose to determine CA adjustments applied to active power by the value of frequency deviations, which greatly simplifies the implementation of the ESS ACS. The reactive power CA is proposed to be performed in line with the principle of excitation boost, which allows not to perform a general reconfiguration of the ACS of active elements in the power supply systems. This makes it possible to prevent GREPs shutdown during short-term frequency and voltage deviations that result from severe disturbances during islanded operation of the power supply system, as well as to ensure reliable power supply of process lines from GREPs, preventing possible damages and losses from the reduced output.

## 6. Method for Maintaining the ESS State of Charge Depending on the Current ESS Load and SoC Values

Depending on the task being solved by the ESS, the SoC value may be different under different circuit diagram configurations and operating conditions. Let us address the issue of maintaining a given level of ESS SoC as applied to solving the problem of preventing GREP shutdowns by frequency protection during its short-term deviations in transients.

In the method developed by the authors for maintaining the SoC of the ESS operating in the *PQ*-control mode, the required SoC value is maintained by changing the slope of the ESS steady-state power frequency characteristic and its offset along the frequency axis depending on the SoC value. In the general case, the steady-state power frequency characteristic is described by the expression:

$$f - f_{\text{nom}} = -K_{\text{ESS}}\,(P_{\text{ESS}} - P_{\text{ESS.0}}), \tag{3}$$

where $f$ is the current frequency value, Hz; $f_{\text{nom}}$ is the nominal frequency, Hz; $K_{\text{ESS}}$ is the ESS droop, Hz/MW; $P_{\text{ESS}}$ is the current active power of the ESS, MW; $P_{\text{ESS.0}}$ is the active power of the ESS at $f_{\text{nom}}$, MW.

The $K_{\text{ESS}}$ factor captures the relationship between the change in frequency and the active power output of the ESS during isolated or islanded operation of the power supply system, as a response to the change in frequency.

The first of the degrees of freedom in Expression (3) is $K_{\text{ESS}}$, which determines the slope angle of the steady-state power frequency characteristic of the ESS. By adding to Expression (3) the factor that takes into account the change in SoC, it is possible to change the $K_{\text{ESS}}$ and, hence, the intensity of the ESS response to the change in frequency at different values of SoC. According to [34,44], assuming $P_{\text{ESS.0}} = 0$, Expression (3) for the charging and discharging modes, respectively, takes the form:

$$f - f_{\text{nom}} = -K_{\text{ESS}} \cdot P_{\text{ESS}} = -\frac{K_{\text{ESS.0}}}{\text{SoC}^n} \cdot P_{\text{ESS}}, P_{\text{ESS}} \geq 0, \tag{4}$$

$$f - f_{\text{nom}} = -K_{\text{ESS}} \cdot P_{\text{ESS}} = -K_{\text{ESS.0}} \cdot \text{SoC}^n \cdot P_{\text{ESS}}, P_{\text{ESS}} \leq 0, \tag{5}$$

where $K_{\text{ESS.0}}$ is the droop of ESS at SoC = 1, Hz/MW, $n$ is the exponent of the power function ($n > 0$).

Let us obtain the current ESS power from Expressions (4) and (5):

$$P_{\text{ESS}} = -\frac{f - f_{\text{nom}}}{K_{\text{ESS.0}}} \cdot \text{SoC}^n,\ P_{\text{ESS}} \geq 0 \text{ (discharging, if } f < f_{\text{nom}};\ \text{SoC} \downarrow), \tag{6}$$

$$P_{\text{ESS}} = -\frac{f - f_{\text{nom}}}{K_{\text{ESS.0}}} \cdot \frac{1}{\text{SoC}^n},\ P_{\text{ESS}} \leq 0 \text{ (charging, if } f > f_{\text{nom}};\ \text{SoC} \uparrow). \tag{7}$$

When the frequency deviates downwards from $f_{\text{nom}}$, the ESS AC generates a power setting of $P_{\text{ESS}} \geq 0$, and the ESS begins to discharge, delivering power to the power supply system. In this case, the available power of the ESS decreases simultaneously with SoC. When the frequency deviates upwards from $f_{\text{nom}}$, the ESS ACS generates a power setting of $P_{\text{ESS}} \leq 0$, ensuring the ESS charge. In this case, the available power of the ESS grows simultaneously with the SoC (Figure 8).

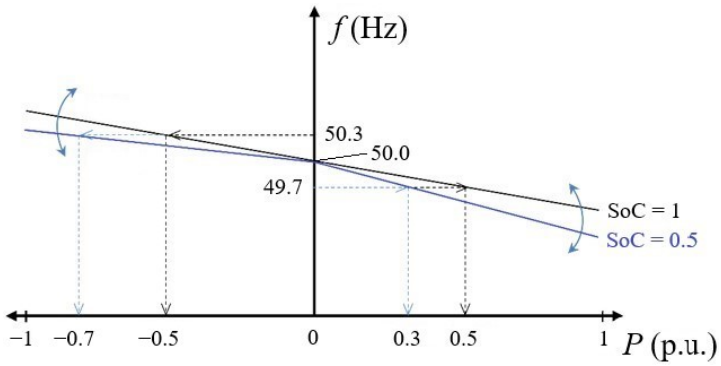


**Figure 8.** Steady-state characteristic *P*(*f*) with SoC-dependent droop.

The exponent *n* in Expressions (6) and (7) has a significant effect on the power of the ESS, depending on SoC. This way of regulating the ESS (minimum response time) can lead to dynamic instability during short-term frequency changes given islanded operation of the power supply system. This should be taken into account when performing transient calculations in the design process. Small values of *n* lead to an insignificant change in the slope of the steady-state power frequency characteristic, with $K_{ESS.0} \approx K_{ESS}$, and with its large values the slope of the steady-state characteristic changes significantly when changing the SoC value.

Figure 9 shows graphs of the sensitivity of $P_{ESS}$ to variations in *n* in the range from 0.1 to 2 at the chosen droop with respect to frequency $K_{ESS.0} = 10^{-6}$ Hz/W as a function of the value of SoC. Figure 9a shows the ESS charging mode with frequency change $f - f_{nom} = 0.5$ Hz, and Figure 9b shows the ESS discharging mode with frequency change $f - f_{nom} = -0.5$ Hz. The power of the ESS is limited by the ACS at 2.5 MW.

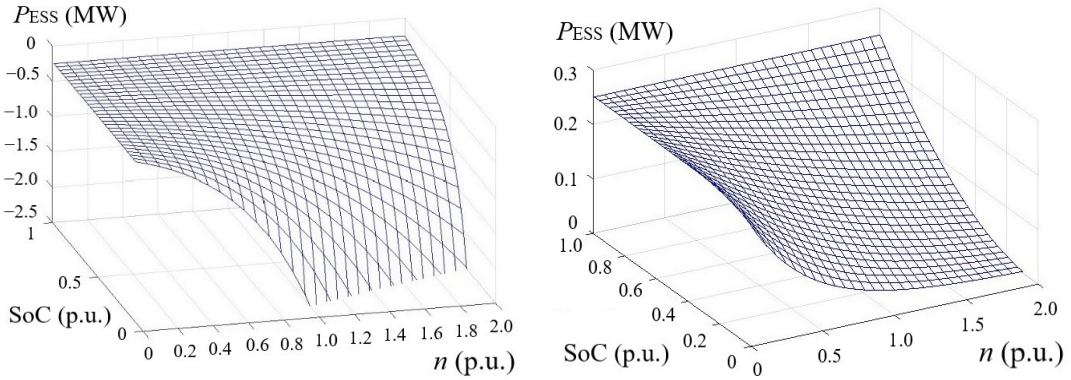


**Figure 9.** Graphs of the sensitivity of $P_{ESS}$ to changes in *n* depending on SoC values: (**a**)—ESS charging mode; (**b**)—ESS discharging mode.

The analysis of Figure 9 shows that as the value of *n* increases, the ESS response to changes in SoC increases significantly, so it is advisable to limit the range of SoC change (set the setpoints), within which the method developed by the authors will be effective.

The second degree of freedom in Expression (3) is the frequency (*f*); therefore, it is possible to offset the steady-state characteristic along the frequency axis by some value $\Delta f$ as a function of the SoC value. In this case, Expressions (6) and (7) for the ESS power take the form:

$$P_{ESS} = -\frac{(f - f_{nom}) - \Delta f}{K_{ESS.0}},\ P_{ESS} \geq 0 \text{ (discharging, if } f < f_{nom}\text{; SoC} \downarrow), \quad (8)$$

$$P_{\text{ESS}} = -\frac{(f-f_{\text{nom}})+\Delta f}{K_{\text{ESS.0}}},\ P_{\text{ESS}} \le 0 \text{ (charging, if } f > f_{\text{nom}};\ \text{SoC} \uparrow). \quad (9)$$

The value of $\Delta f$ can depend linearly on the SoC, as in Expression (10), be set as a fixed value depending on the current value of the SoC, or have the form of a piecewise linear function.

$$\Delta f = m_{\text{SoC}}\ (\text{SoC} - \text{SoC}_{\text{set}}), \quad (10)$$

where $m_{\text{SoC}}$ is the coefficient of proportionality; $\text{SoC}_{\text{set}}$ is the SoC setpoint value.

When the ESS is discharged, the static frequency characteristic should gradually shift downward along the frequency axis, causing the ESS discharge power to decrease linearly, and when in the case of charging it should shift upward, causing the charge power to increase, as shown in Figure 10.

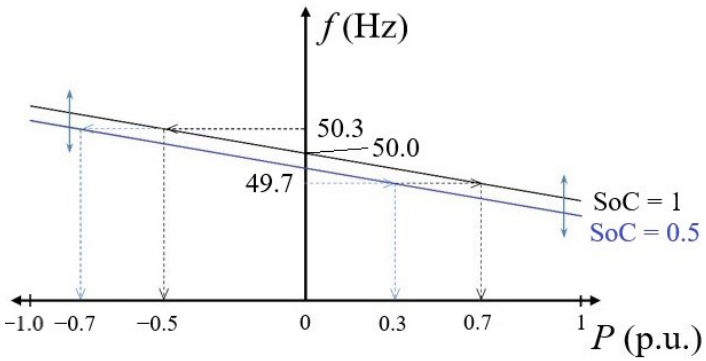


**Figure 10.** Steady-state characteristic $P(f)$ offset along the frequency axis depending on the SoC value of the ESS.

An analysis of the sensitivity of the $P_{\text{ESS}}$ to changes in $m_{\text{SoC}}$ is not presented in the article, but it should be noted that the maximum value of $\Delta f$ should not be greater than the actual frequency deviation in the islanded operation of the power supply system. Otherwise, there may be a sharp shift of the operating point of the characteristic to the area of the opposite mode of operation of the ESS. In this case, the ESS ACS will form an incorrect command (for example, the command to charge instead of discharge) and the parameters of the operating condition will go beyond the range of permissible values, which is unacceptable.

Based on the results of the analysis of the features of the steady-state characteristic offset depending on the value of SoC, the ESS power regulation was assumed to be in accordance with Expressions (11) and (12), aimed at stabilizing the frequency and maintaining SoC within a given range.

$$P_{\text{ESS}} = -\frac{(f-f_{\text{nom}})-\Delta f}{K_{\text{ESS.0}}} \cdot \text{SoC}^n,\ P_{\text{ESS}} \ge 0 \text{ (discharging, if } f < f_{\text{nom}};\ \text{SoC} \downarrow) \quad (11)$$

$$P_{\text{ESS}} = -\frac{(f-f_{\text{nom}})+\Delta f}{K_{\text{ESS.0}}} \cdot \frac{1}{\text{SoC}^n},\ P_{\text{ESS}} \le 0 \text{ (charging, if } f > f_{\text{nom}};\ \text{SoC} \uparrow) \quad (12)$$

For effective frequency control in the case of islanded operation of the power supply system with GREPs, the range of power variation of the ESS in both directions should be the greatest possible, which is usually achievable at SoC = 0.5 (50%). Regardless of the control algorithms specified in the ESS ACS, there is an optimal SoC range for frequency control purposes, whose boundaries it is not recommended to exceed [50].

Deep cycling of the ESS battery storage as well as regular charging to 100% reduces the calendar and cycling life of the battery storage, which is expressed in a premature loss of energy capacity [51]. Therefore, the ESS should operate within the optimal SoC range with a steady-state power frequency characteristic offset depending on the SoC value, as recommended in [43]. Additionally, it is reasonable to change the slope of the steady-state

characteristic depending on the SoC in the regions of the upper and lower limit states of the ESS SoC, as shown in Figure 11.

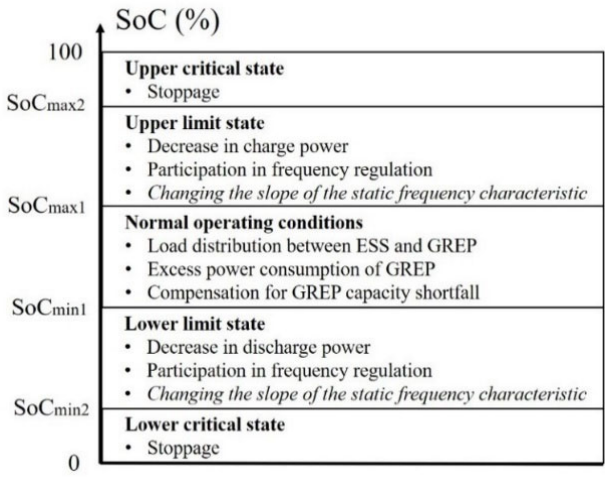


**Figure 11.** Graph of the division of the range of SoC values into areas of ESS operation.

The $\Delta f$ quantity in Expressions (11) and (12) is determined by a piecewise linear function:

$$\Delta f = \begin{cases} -P_{\mathrm{ESS}} \cdot R, \mathrm{SoC} \geq \mathrm{SoC}_{\mathrm{max2}}, \\ f_{\max} - f_{\mathrm{lim.max}}, \mathrm{SoC}_{\mathrm{max1}} \leq \mathrm{SoC} \leq \mathrm{SoC}_{\mathrm{max2}}, \\ 0, \mathrm{SoC}_{\mathrm{min1}} \leq \mathrm{SoC} \leq \mathrm{SoC}_{\mathrm{max1}}, \\ f_{\min} - f_{\mathrm{lim.min}}, \mathrm{SoC}_{\mathrm{min2}} \leq \mathrm{SoC} \leq \mathrm{SoC}_{\mathrm{min1}}, \\ -P_{\mathrm{ESS}} \cdot R, \mathrm{SoC} \leq \mathrm{SoC}_{\mathrm{min2}}, \end{cases} \quad (13)$$

where $R$—droop with respect to frequency for the GREP generator; $f_{\max}/f_{\min}$—critical maximum/minimum frequency value; $f_{\mathrm{lim.max}}/f_{\mathrm{lim.min}}$—maximum/minimum frequency offset limit.

Changing the slope angle of the steady-state characteristic in the regions of upper and lower limit states of the SoC strengthens the response of the ESS in the right direction as the SoC approaches them.

Figure 12 shows a general view of the segmented steady-state characteristic of the ESS with an offset along the frequency axis and a change in the droop depending on the SoC value (black line—steady-state characteristic of the GREP; green line—steady-state characteristic of the ESS divided into sections at SoC = 0.5; vertical section on the frequency axis—dead band of the ESS frequency control algorithm).

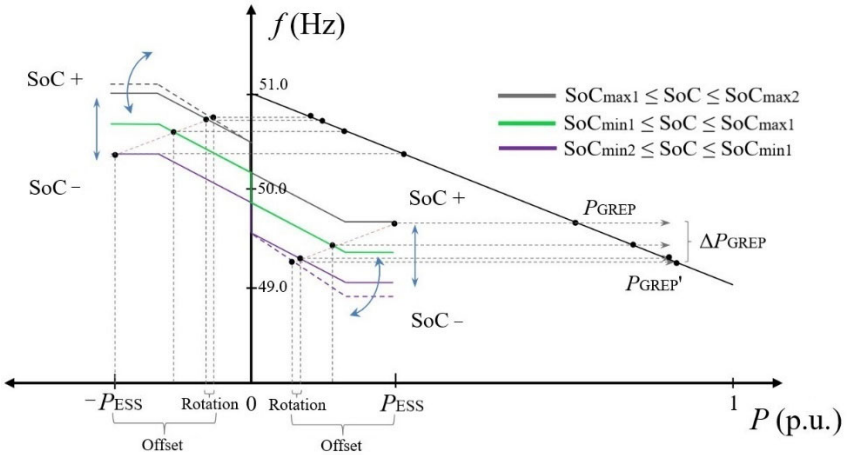


**Figure 12.** Segmented steady-state characteristic of the ESS.

In the inclined sections of the characteristic (Figure 12), the power is distributed between the GREP and the ESS, while in the horizontal sections, the ESS power is maintained so as to ensure constant delivery of the maximum permissible power of the GREP, preventing its emergency shutdown. When the ESS is discharged, the steady-state characteristic gets offset upwards, and when it is charged, it gets offset downwards by $\Delta f$. When the lower or upper limit state of the SoC is reached, the slope of the steady-state power frequency characteristic of the ESS changes to increase the discharge power at high SoC values or decrease it at low SoC values. The movement of the operating points of the ESS and GREP in Figure 12 can be traced by the gray dashed lines. A detailed description of the frequency regulator can be found in [43].

The method developed by the authors for maintaining the SoC of the GREP does not require the availability of a data link between the ESS and the GREP. This method consists in dividing the steady-state power/frequency characteristic into sections with different droops that are chosen depending on the current load of the ESS and the battery state of charge and offsetting it according to a specified pattern. This makes it possible during islanded operation of a power supply system of an industrial facility with GREPs to ensure reliable operation of the ESS, preserving the calendar and cycling service life of the battery storage, as well as preventing premature loss of its power capacity.

## 7. Conclusions

GREPs shutdowns by process protections or protective relays under severe disturbances in the islanded operation of power supply systems of industrial facilities lead to damages and losses due to load shedding. GREPs shutdowns can be prevented by using ESSs to compensate for instantaneous imbalances of active and reactive power, accompanied by short-term frequency and/or voltage deviations during transients.

The most severe disturbances during islanded operation are large surges of load on GREPs due to one of them being switched off, the group starting of electric motors, and load shedding (more than 50%) during short circuits or disconnection of process lines.

The method developed by the authors for independent control of active and reactive power output/consumption of the ESS does not require the online calculation of CA adjustments at the ESS. We propose to determine CA adjustments applied to active power by the value of frequency deviations, which greatly simplifies the implementation of the ESS ACS. Optimal values of frequency control time intervals and CA adjustments at the ESS are chosen based on the results of calculations of electromechanical transients. We propose to perform the reactive power control in line with the principle of excitation boost, which allows one not to perform a general reconfiguration of the ACS of active elements in the power supply systems, providing good damping of oscillations in case of emergency disturbances.

The method developed by the authors for maintaining the SoC of the GREP does not require the availability of a data link between the ESS and the GREP. This method consists in dividing the steady-state power/frequency characteristic into sections with different droops that are chosen depending on the current load of the ESS and the battery state of charge and offsetting it according to a specified pattern. This helps to preserve the calendar and cycling lifetime of the ESS BS, preventing premature loss of its energy capacity.

The methods developed by the authors for intelligent ESS control allow one to prevent GREPs from switching off during islanded operation, even under severe disturbances, which is proved by the results of calculations of electromechanical transients. This makes it possible to ensure a reliable power supply of process lines at industrial facilities from GREPs, preventing possible damage from their shutdowns and losses from the reduced output.

**Author Contributions:** Conceptualization, P.I. and A.K.; methodology, S.F.; software, P.I.; validation, K.S. and D.K.; formal analysis, A.K.; data curation, K.S.; writing—original draft preparation,

P.I.; writing—review and editing, K.S.; visualization, D.K.; supervision, A.K.; project administration, S.F. All authors have read and agreed to the published version of the manuscript.

**Funding:** This work is supported by the Russian Science Foundation under grant 21-79-30013 in the Energy Research Institute of the Russian Academy of Sciences.

**Institutional Review Board Statement:** Not applicable.

**Informed Consent Statement:** Not applicable.

**Data Availability Statement:** Data sharing is not applicable. No new data were created or analyzed in this study. Data sharing is not applicable to this article.

**Conflicts of Interest:** The funders had no role in the design of the study; in the collection, analysis, or interpretation of data; in the writing of the manuscript, or in the decision to publish the results.

## Abbreviations

| | |
|---|---|
| GREP | Gas-fired reciprocating engine plant |
| ESS | Energy storage system |
| PR | Protective relay |
| SoC | State of charge |
| BS | Battery storage |
| SC | Short-circuit |
| AR | Automatic reclosing |
| ATS | Automatic transfer switches |
| ACS | Automatic control systems |
| UFLS | Under-frequency load shedding |
| CA | Control actions |
| LS | Load shedding |
| SALSS | Special automatic load shedding system |
| EMF | Electromotive force |
| IPB | Infinite power bus |

## References

1. Zhang, H. Technology innovation, economic growth and carbon emissions in the context of carbon neutrality: Evidence from BRICS. *Sustainability* **2021**, *13*, 11138. http://dx.doi.org/10.3390/su132011138.
2. Dong, F.; Qin, C.; Zhang, X.; Zhao, X.; Pan, Y.; Gao, Y.; Zhu, J.; Li, Y. Towards carbon neutrality: The impact of renewable energy development on carbon emission efficiency. *Int. J. Environ. Res. Public Health* **2021**, *18*, 13284. https://doi.org/10.3390/ijerph182413284.
3. Lin, J.; Shen, Y.; Li, X.; Hasnaoui, A. BRICS carbon neutrality target: Measuring the impact of electricity production from renewable energy sources and globalization. *J. Environ. Manag.* **2021**, *298*, 113460. http://dx.doi.org/10.1016/j.jenvman.2021.113460.
4. Ilyushin, P.V.; Pazderin, A.V.; Seit, R.I. Photovoltaic power plants participation in frequency and voltage regulation. In Proceedings of the 17th International Ural Conf. on AC Electric Drives (ACED 2018), Ekaterinburg, Russia, 26–30 March 2018. https://doi.org/10.1109/ACED.2018.8341712.
5. Singh, B.; Sharma, J. A review on distributed generation planning. *Renew. Sustain. Energy Rev.* **2017**, *76*, 529–544. https://doi.org/10.1016/J.RSER.2017.03.034.
6. Mehigana, L.; Deanea, J.P.; Gallachóira, B.P.Ó.; Bertsch, V. A review of the role of distributed generation (DG) in future electricity systems. *Energy* **2018**, *163*, 822–836. http://dx.doi.org/10.1016/j.energy.2018.08.022.
7. Kretov, D.; Kostyukov, V. The Economic Efficiency of an Off-Grid Power Sources Implementation Based on A Medium Power Gas-Fired Reciprocating Units. In Proceedings of the 2021 International Conference on Electrotechnical Complexes and Systems (ICOECS), Ufa, Russia, 16–18 November 2021. https://doi.org/10.1109/ICOECS52783.2021.9657478.
8. Zhidko, A. Using Electromagnetic Continuously Variable Transmission in Gas Reciprocating Power Plant to Ensure Dynamic Stability. In Proceedings of the 2020 International Conference on Industrial Engineering, Applications and Manufacturing (ICIEAM), Sochi, Russia, 18–22 May 2020.
9. Ilyushin, P.; Kulikov, A.; Suslov, K.; Filippov, S. Consideration of Distinguishing Design Features of Gas-Turbine and Gas-Reciprocating Units in Design of Emergency Control Systems. *Machines* **2021**, *9*, 47. https://doi.org/10.3390/machines9030047.
10. Papkov, B.; Gerhards, J.; Mahnitko, A. System problems of power supply reliability analysis formalization. In Proceedings of the 2015 IEEE 5th International Conference on Power Engineering, Energy and Electrical Drives, Riga, Latvia, 11–13 May 2015; pp. 225–228. https://doi.org/10.1109/PowerEng.2015.7266324.
11. Praiselin, W.J.; Edward, J.B. A review on impacts of power quality, control and optimization strategies of integration of renewable energy based microgrid operation. *Int. J. Intell. Syst. Appl.* **2018**, *10*, 67–81. http://dx.doi.org/10.5815/IJISA.2018.03.08.

12. Ilyushin, P.V.; Pazderin, A.V. Approaches to organization of emergency control at isolated operation of energy areas with distributed generation. In Proceedings of the International Ural Conference on Green Energy, Chelyabinsk, Russia, 4–6 October 2018. https://doi.org/10.1109/URALCON.2018.8544361.
13. Karamov, D.N. Autonomous renewable energy systems in Russia. Critical review of the current situation. *Energy Rep.* **2020**, *6*, 31–37. https://doi.org/10.1016/j.egyr.2020.10.033.
14. Petrovskaia, T.K.; Frolova, Y.A.; Frolov, M.Y. The Online Method of Input/Output Unified GAS Reciprocating Generation Unit in Island Mode. In Proceedings of the 2018 XIV International Scientific-Technical Conference on Actual Problems of Electronics Instrument Engineering (APEIE), Novosibirsk, Russia, 2–6 October 2018. https://doi.org/10.1109/APEIE.2018.8545788.
15. Sharygin, M.; Vukolov, V.; Petrov, A. Adaptive multivariable relay protection of reconfigurable distribution networks. In Proceedings of the Rudenko International Conference "Methodological Problems in Reliability Study of Large Energy Systems", RSES 2019, Tashkent, Uzbekistan, 23–27 September 2019; E3S Web of Conferences, Article Number 01048.
16. Ilyushin, P.V.; Pazderin, A.V. Requirements for power stations islanding automation an influence of power grid parameters and loads. In Proceedings of the 2018 International Conference on Industrial Engineering, Applications and Manufacturing (ICIEAM), Moscow, Russia, 15–18 May 2018.
17. Papkov, B.; Osokin, V. Reliability assessment of electric power system with distributed generation facilities. *Energy Syst. Research* **2020**, *3*, 62–69.
18. He, W.; King, M.; Luo, X.; Dooner, M.; Li, D.; Wang, J. Technologies and economics of electric energy storages in power systems: Review and perspective. *Adv. Appl. Energy* **2021**, *4*, 100060. https://doi.org/10.1016/j.adapen.2021.100060.
19. Jafaria, M.; Botteruda, A.; Sakti, A. Decarbonizing power systems: A critical review of the role of energy storage. *Renew. Sustain. Energy Rev.* **2022**, *158*, 112077. https://doi.org/10.1016/j.rser.2022.112077.
20. Yang, B.; Wang, J.; Chen, Y.; Li, D.; Zeng, C.; Chen, Y.; Guo, Z.; Shu, H.; Zhang, X.; Yu, T.; et al. Optimal sizing and placement of energy storage system in power grids: A state-of-the-art one-stop handbook. *J. Energy Storage* **2020**, *32*, 101814. https://doi.org/10.1016/j.est.2020.101814.
21. Premadasa, P.N.D.; Chandima, D.P. An innovative approach of optimizing size and cost of hybrid energy storage system with state of charge regulation for stand-alone direct current microgrids. *J. Energy Storage* **2020**, *32*, 101703. https://doi.org/10.1016/j.est.2020.101703.
22. Lia, J.; Zou, W.; Yang, Q.; Yi, F.; Bai, Y.; Wei, Z.; He, H. Size optimization and power allocation of a hybrid energy storage system for frequency service. *Int. J. Electr. Power Energy Syst.* **2022**, *141*, 108165. https://doi.org/10.1016/j.ijepes.2022.108165.
23. Ilyushin, P.V.; Suslov, K.V. Operation of automatic transfer switches in the networks with distributed generation. In Proceedings of the 2019 IEEE Milan PowerTech, Milan, Italy, 23–27 June 2017. https://doi.org/10.1109/PTC.2019.8810450.
24. Gurevich, Y.E.; Libova, L.E. *Application of Mathematical Models of Electrical Load in Calculation of the Power Systems Stability and Reliability of Power Supply to Industrial Enterprises*; ELEKS-KM: Moscow, Russia, 2008. (In Russian)
25. Gurevich, Y.E.; Kabikov, K.V. *Peculiarities of Power Supply, Aimed at Failure-Free Operation of Industrial Consumers*; ELEKS-KM: Moscow, Russia, 2005. (In Russian)
26. Sharygin, M.V.; Kulikov, A.L. Statistical methods of mode recognition in relay protection and automation of power supply networks. *Power Technol. Eng.* **2018**, *52*, 235–241.
27. Ghadi, M.; Rajabi, A.; Ghavidel, S.; Azizivahed, A.; Li, L.; Zhang, J. From active distribution systems to decentralized microgrids: A review on regulations and planning approaches based on operational factors. *Appl. Energy* **2019**, *253*, 113543.
28. Begovic, M.M. (Ed.) *Electrical Transmission Systems and Smart Grids: Selected Entries from the Encyclopedia of Sustainability Science and Technology*; Springer Science+Business Media: New York, NY, USA, 2013.
29. Lin, X.; Zamora, R. Controls of hybrid energy storage systems in microgrids: Critical review, case study and future trends. *J. Energy Storage* **2022**, *47*, 103884. https://doi.org/10.1016/j.est.2021.103884.
30. Nesterenko, G.; Prankevich, G.; Eroshenko, S.; Chuvashev, R.; Zyryanov, V. Technical and economic efficiency analysis of the energy storage systems use in off-grid power systems. In Proceedings of the 7th International Conference on Electrical Energy Systems (ICEES), Virtual, 11–13 February 2021; pp. 68–72. https://doi.org/10.1109/ICEES51510.2021.9383742.
31. Rocabert, J.; Luna, A.; Blaabjerg, F.; Rodriguez, P. Control of power converters in AC Microgrids. *IEEE Trans. Power Electron.* **2012**, *27*, 4734–4749.
32. Unruh, P.; Nuschke, M.; Strauss, P.; Welck, F. Overview on grid-forming inverter control methods. *Energies* **2020**, *13*, 2589. https://doi.org/10.3390/en13102589.
33. Khodadoost, A.A.; Gharehpetian, G.B.; Abedi, M. Review on energy storage systems control methods in microgrids. *Int. J. Electr. Power Energy Syst.* **2019**, *107*, 745–757.
34. Gao, D.W. Chapter 1. Basic concepts and control architecture of microgrids. In *Energy Storage for Sustainable Microgrid*; Academic Press: Cambridge, MA, USA, 2015; 152p.
35. Kim, Y.S.; Kim, E.S.; Moon, S. Frequency and voltage control strategy of standalone microgrids with high penetration of intermittent renewable generation systems. *IEEE Trans. Power Syst.* **2015**, *31*, 718–728. https://doi.org/10.1109/TPWRS.2015.2407392.
36. Kim, Y.S.; Hwang, C.S.; Kim, E.S.; Cho, C. State of charge-based active power sharing method in a standalone microgrid with high penetration level of renewable energy sources. *Energies* **2016**, *9*, 480. https://doi.org/10.3390/en9070480.
37. Lu, X.; Sun, K.; Guerrero, J.M.; Huang, L. SoC-based dynamic power sharing method with AC-bus voltage restoration for microgrid applications. In Proceedings of the 38th Annual Conference on IEEE Industrial Electronics Society (IECON), Montreal, QC, Canada, 25–28 October 2012, pp. 5677–5682. https://doi.org/10.1109/IECON.2012.6389058.

38. Gkavanoudis, S.I.; Oureilidis, K.; Demoulias, C.S. An adaptive droop control method for balancing the SoC of distributed batteries in AC microgrids. In Proceedings of the IEEE 17th Workshop on Control and Modeling for Power Electronics (COMPEL), Trondheim, Norway, 27–30 June 2016; pp. 1–6. https://doi.org/10.1109/COMPEL.2016.7556698.
39. Wang, R.; Sun, Q.; Hu, W.; Li, Y.; Ma, D.; Wang, P. SoC-based droop coefficients stability region analysis of the battery for stand-alone supply systems with constant power loads. *IEEE Trans. Power Electron.* **2021**, *36*, 7866–7879. https://doi.org/10.1109/TPEL.2021.3049241.
40. Duc, N.H. An innovative adaptive droop control based on available energy for DC micro distribution grids. *Energies* **2020**, *13*, 2983. https://doi.org/10.3390/en13112983.
41. Lu, X.; Sun, K.; Guerrero, J.M.; Vasquez, J.C.; Huang, L.; Teodorescu, R. SoC-based droop method for distributed energy storage in DC microgrid applications. In Proceedings of the IEEE International Symposium on Industrial Electronics (ISIE), Hangzhou, China, 28–31 May 2012; pp. 1640–1645. https://doi.org/10.1109/ISIE.2012.6237336.
42. Yang, H.; Qiu, Y.; Li, Q.; Chen, W. A self-convergence droop control of no communication based on double-quadrant state of charge in DC microgrid applications. *J. Renew. Sustain. Energy* **2017**, *9*, 034102. https://doi.org/10.1063/1.4985092.
43. Sitompul, S.; Hanawa, Y.; Bupphaves, V.; Fujita, G. State of charge control integrated with load frequency control for BESS in islanded microgrid. *Energies* **2020**, *13*, 4657. https://doi.org/10.3390/en13184657.
44. Urtasun, A.; Sanchis, P.; Marroyo, L. State-of-charge-based droop control for stand-alone AC supply systems with distributed energy storage. *Energy Convers. Manag.* **2015**, *106*, 709–720. https://doi.org/10.1016/j.enconman.2015.10.010.
45. Shim, J.W.; Verbic, G.; Kim, H.; Hur, K. On droop control of energy-constrained battery energy storage systems for grid frequency regulation. *IEEE Access* **2019**, *7*, 166353–166364. https://doi.org/10.1109/ACCESS.2019.2953479.
46. Ilyushin, P.V.; Shepovalova, O.V.; Filippov, S.P.; Nekrasov, A.A. Calculating the sequence of stationary modes in power distribution networks of Russia for wide-scale integration of renewable energy-based installations. *Energy Rep.* **2021**, *7*, 308–327.
47. Ilyushin, P.; Filippov, S.; Kulikov, A. Effective energy storage power control to extend the acceptable range of generator frequency in distributed generation. *E3S Web Conf.* **2021**, *288*, 01006. https://doi.org/10.1051/e3sconf/202128801006.
48. Shushpanov, I.; Suslov, K.; Ilyushin, P.; Sidorov, D. Towards the flexible distribution networks design using the reliability performance metric. *Energies* **2021**, *14*, 6193. https://doi.org/10.3390/en14169854.
49. Alberto Escalera, A.; Prodanović, M.; Castronuovo, E.D. Analytical methodology for reliability assessment of distribution networks with energy storage in islanded and emergency-tie restoration modes. *Int. J. Electr. Power Energy Syst.* **2019**, *107*, 735–744.
50. Zeh, A.; Müller, M.; Naumann, M.; Hesse, H.C.; Jossen, A.; Witzmann, R. Fundamentals of using battery energy storage systems to provide primary control reserves in Germany. *Batteries* **2016**, *2*, 29. https://doi.org/10.3390/batteries2030029.
51. Swierczynski, M.; Stroe, D.I.; Stan, A.I.; Teodorescu, R.; Kær, S.K. Lifetime estimation of the nanophosphate LiFePO4/C battery chemistry used in fully electric vehicles. *IEEE Trans. Ind. Appl.* **2015**, *51*, 3453–3461. https://doi.org/10.1109/TIA.2015.2405500.